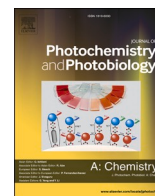




Contents lists available at ScienceDirect

Journal of Photochemistry & Photobiology, A: Chemistry

journal homepage: www.elsevier.com/locate/jphotochem

Blue-red emitting 2,12-disubstituted [5]helicenes for high fluorescence efficiency and sensing application

B. Yadagiri^{a,b}, Prem Jyoti Singh Rana^a, Surya Prakash Singh^{a,b,*}^a Polymers and Functional Materials Division, CSIR-Indian Institute of Chemical Technology, Uppal Road, Tarnaka, Hyderabad, 500007, India^b Academy of Scientific and Innovative Research (AcSIR), Ghaziabad, Uttar Pradesh, India

ARTICLE INFO

Keywords:

Helicene

Fluorophores

Dual application

Sensing application

Security application

ABSTRACT

We report photochemical synthesis of two new fluorene and carbazole-based 2,12-disubstituted [5]helicenes namely FLU-HEL and CBZ-HEL respectively. Both FLU-HEL and CBZ-HEL exhibit very intense fluorescence property in solution as well as solid state. The fluorescence quantum yield (Φ_f) = 27 % and 30 % and life time (τ_f) = 9.7 ns and 4.2 ns were observed for both [5]helicenes, respectively. Also, both the [5]helicene dyes have shown very good sensing properties towards Fe^{3+} transition metal ion than other transition metal ions. We have also explored the feasibility of these compounds for security applications.

1. Introduction

Organic molecules with extended delocalized π -electron systems have been extensively used for fluorescence and non-linear applications. Generally high fluorescence phenomenon occurs by the electron donating and electron withdrawing groups [1]. Even though a number of organic dyes show intense fluorescence in solution state, only a few reports are available on full-colour emission organic dyes both in solution and solid state [2]. This is due to the quenching of the fluorescence arising from the presence of intermolecular interaction and aggregation of molecular assembly [3].

To improve the fluorescence behaviour and resolve above mentioned demerits of organic dyes, several approaches were adopted i.e. J-aggregate formation [4], enhanced intramolecular charge transfer transition [5], and aggregation induced emission for the development of new small molecular organic dyes [6]. In yet another approach, the full-colour emission spectra can be achieved by systematic design of a molecule via incorporation of the various chromophores at different positions to the molecular backbone of organic dyes [7].

Helically ortho-fused polyaromatic hydrocarbons are generally referred as helicenes [8]. The recent reports show that [5]helicene based organic materials display intense fluorescence behaviour in both solution and solid state. In Fig. 1 we have shown some [5]helicenes and its analogues reported earlier and investigated by us in the present work [9].

Recently, Chuan-Feng Chen et al. reported a new tetrahydro[5]helicene based imides dye having intense fluorescence and large Stokes shifts in both solution and solid state (Fig. 1; A and B) [10]. Kenji Matsuda and co-workers demonstrated the fluorescence properties of 5, 10-disubstituted [5]helicene derivative (Fig. 1; C) in solutions state and its self-assembly behaviours [9]. Further, Julian M. W. Chan et al., reported sultam-based hetero[5]helicene for a typical blue shifting of its solid state emission relative to the solution phase (Fig. 1; D).

The fluorescence phenomenon also useful for the sensitive detection of micro levels of analysing agents such as small molecules, anions and cations. A fluorescence sensor consists of two parts, ionophore and fluorophore. The ionophore has binding ability towards analyte and fluorophore emits the fluorescence signal. Recently, [5]helicene based organic dyes gained good attention as a fluorescence sensors in biological and other applications, because of its chiral structure and more π -electron cloud on the molecular backbone [11–13]. The development of fluorescent probes that were used for the sensing of different hazardous chemicals and elements in living cells is important, because the abnormal production of hazardous chemicals and elements can damage cellular biomolecules, which was closely connected with numerous diseases [21–23]. Previously some research groups reported applications of [5]helicenes for sensing metal ions and discuss about their binding phenomenon [16]. Nantanit Wanichacheva et al. developed a [5]helicene derivative for water-soluble Fe^{3+} fluorescence sensor with a large Stokes shift (192 nm) [13]. This helicene based sensor was used to

* Corresponding author at: Polymers and Functional Materials Division, CSIR-Indian Institute of Chemical Technology, Uppal Road, Tarnaka, Hyderabad, 500007, India.

E-mail address: spsingh@iict.res.in (S.P. Singh).

<https://doi.org/10.1016/j.jphotochem.2021.113203>

Received 4 November 2020; Received in revised form 23 January 2021; Accepted 6 February 2021

Available online 12 February 2021

1010-6030/© 2021 Elsevier B.V. All rights reserved.

identify Fe^{3+} in human cancer cells. In this work, we have developed [5]helicene based sensors for Fe^{3+} ion sensing property and security applications.

Herein, we describe the design and synthesis by the photocyclodehydrogenation reaction of two novel symmetric 2,12-disubstituted [5]helicenes namely 9,12-bis(9,9-dioctyl-9H-fluorene-2-yl)dibenzo[c,g]phenanthrene-1,6-dicarbonitrile (FLU-HEL) and 9,12-bis(9-octyl-9H-carbazol-3-yl)dibenzo[c,g]phenanthrene-1,6-dicarbonitrile (CBZ-HEL) (Fig. 1). These materials have an ability to show good quantum yield ($\Phi_f = 27\%$ and 30%) and excellent sensing and security applications. These symmetric [5]helicene based organic dyes were substituted with fluorene (FLU-HEL) and carbazole (CBZ-HEL) at 2,12 positions of the [5]helicene skeleton along with substitution of two cyano (-CN) groups at selected positions, respectively. In addition, aliphatic alkyl chains have also been appended to increase the solubility of helicene dyes in all common organic solvents, which is beneficial to study the different applications in different solvents. With this study, we analysed that the substitution on 2,12 positions at [5]helicene core moiety with fluorene and carbazole chromophores can boost the fluorescence performance of [5]helicene at monomeric state.

2. Results and discussion

2.1. Experimental section

General Methods: All reagents from commercial sources were used without further purification unless otherwise noted. Tetrahydrofuran (THF) and 1,4-dioxane were purchased from Alfa Aesar, dried over sodium/benzophenone, distilled under nitrogen and stored over 4 Å molecular sieves. Chloroform (CHCl_3) and dichloroethane (DCE), were dried over calcium hydride (CaH_2), distilled under nitrogen and stored over molecular sieves (4 Å). *N,N*-dimethylformamide (DMF) was dried and purified using standard techniques. Reactions were carried out under a nitrogen atmosphere; Glass TLC plate Silica gel 60G F254 from Merck Millipore was used to monitor the reaction. Compounds were detected by UV irradiation, staining with I_2 and/or KMnO_4 . ^1H and ^{13}C nuclear magnetic resonance (NMR) spectroscopy spectra were recorded on a Bruker Avance-300 MHz, Avance-400 MHz and Avance-500 MHz

spectrometer at 25 °C unless otherwise noted. ^1H and ^{13}C NMR spectra are referenced to SiMe_4 using the residual solvent peak impurity of the solvent CDCl_3 and corresponding data described as follows: chemical shift in parts per million (PPM) measured from tetramethylsilane (TMS) referenced and CDCl_3 ($\delta = 7.26$ ppm) as a residual isotopomer solvent, multiplicity, integration. ^{13}C NMR spectra analysis also well studied by using 400 MHz and corresponding data described as follows: chemical shift in PPM from TMS reference and CDCl_3 ($\delta = 77.16$ ppm). Mass details of synthesized molecules were obtained by high resolution mass spectra such as electrospray ionization (ESI), MALDI-TOF mass and high resolution mass spectrometry (HRMS).

2.2. Synthesis

Synthetic pathways of FLU-HEL and CBZ-HEL are represented in Scheme 1. Synthetic procedure for both [5]helicene dyes is nearly similar. The compounds 1 and 2 were subjected to Miyaura borylation reaction to give compound 3 and 4, followed by compounds 3 and 4 were subjected to Suzuki-Miyaura cross-coupling reaction to obtain compound 5 and 6. Further, the compound 5 and 6 was reacted with terephthalaldehyde in the presence of ethanol via Knoevenagel condensation reaction to get compound 7 and 8. Finally, the target compound 9 and 10 was prepared via photocyclodehydrogenation reaction by using compound 7, 8 and iodine (I_2) in dry toluene under irradiation of 450 nm high-pressure mercury lamp in very good yield [15].

2-Bromo-9,9-dioctyl-9H-fluorene (1): A dry flask (100 mL) was charged with 2-bromofluorene (3.0 g, 0.012 mol), KOH (4.12 g, 0.073 mol) and DMSO (30 mL) under nitrogen gas atmosphere. After stirred for 20 min, 1-bromooctane (7.09 g, 0.036 mol) was slowly added and stirred at 110 °C for 24 h. After completion of the reaction, the reaction mixture was diluted with ice-water/ water (more than two times) and extracted with EtOAc by separatory funnel. The combined organic layer was washed with brine and dried over anhydrous sodium sulphate (Na_2SO_4) and then the organic solvents were completely removed by rotary evaporation. The residue was purified by column chromatography using petroleum as eluent, to afford product 1 yield (5 g, 75%). ^1H NMR (400.1 MHz, CDCl_3): δ 7.67–7.63 (m, 1H), 7.54 (d, 1H), 7.45–7.42 (m, 2H), 7.32–7.28 (m, 3H), 1.98–1.86 (m, 4H),

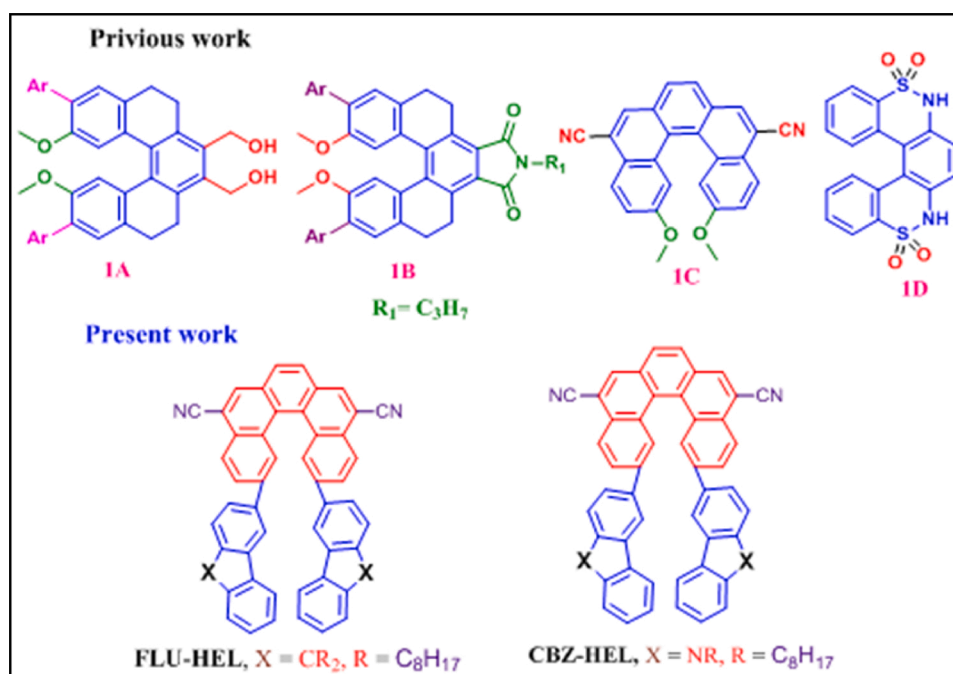
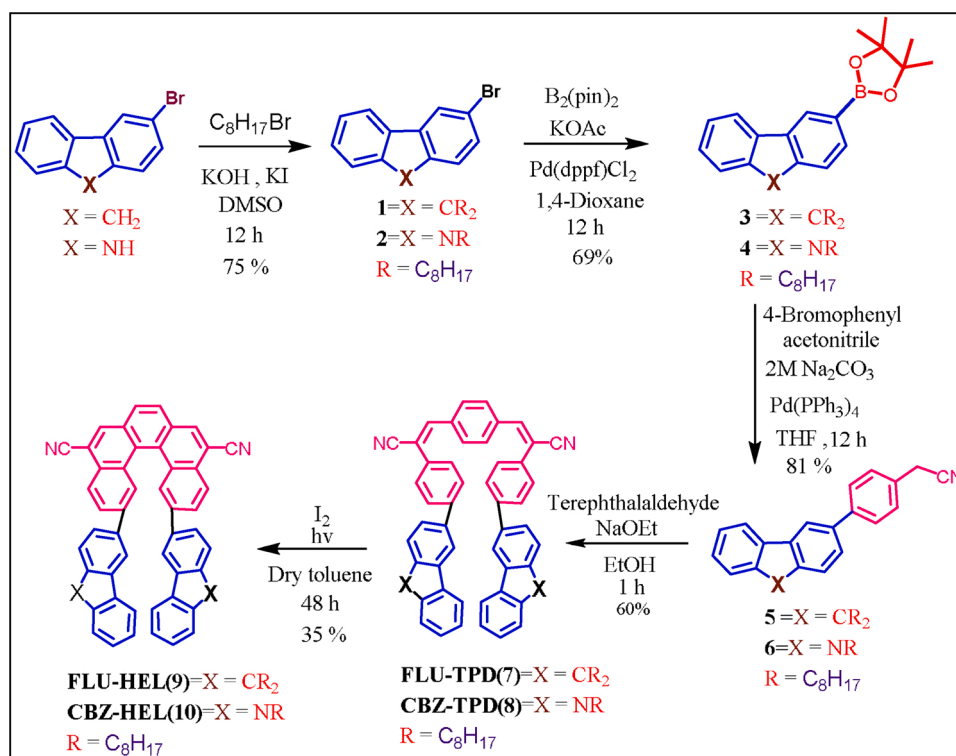


Fig. 1. Previous and present work of [5]helicenes.



Scheme 1. Synthetic route for the preparation of FLU-HEL and CBZ-HEL [5]helicene dyes.

1.32–1.16 (m, 6 H), 1.16–0.98 (m, 18 H), 0.82 (t, 6 H). ^{13}C (75.4 MHz, CDCl_3): δ 152.9, 150.5, 140.1, 140.0, 129.8, 127.4, 126.9, 126.1, 122.9, 121.0, 119.7, 55.4, 40.3, 31.9, 29.9, 29.2, 23.7, 22.6, 14.1. MALDI-TOF-MS m/z $[\text{M}+\text{H}]^+$ calcd for $\text{C}_{29}\text{H}_{41}\text{Br}$ $[\text{M}+\text{H}]^+$ m/z 468.54; found 468.11.

2-(9,9-Dioctyl-9H-fluoren-2-yl)-4,4,5,5-tetramethyl-1,3,2-dioxaborolane (3): To a dry flask (100 mL) was charged with compound 1 (4.65 g, 0.009 mol), Bis(pinacolato)diboron (3.27 g, 0.011 mol), and KOAc (5.82 g, 0.054 mol) in 1,4-dioxane (50 mL), $\text{Pd}(\text{dppf})\text{Cl}_2$ (10 %) was added. The reaction mixture was stirred under nitrogen atmosphere at 100 °C for 24 h. After cooling to room temperature, the solvent was removed under reduced pressure. The residue was purified by column chromatography using silica gel with petroleum ether/ethyl acetate (2:3) to give 3 as colourless liquid yield (3.5 g, 69 %). ^1H NMR (500.1 MHz, CDCl_3): δ 7.82 (d, $J=7.8$ Hz, 1 H), 7.76–7.65 (m, 3 H), 7.37–7.27 (m, 3 H), 2.02–1.90 (m, 4 H), 1.38 (s, 12 H), 1.34–1.14 (m, 4 H), 1.14–0.85 (m, 16 H), 0.80 (s, 6 H). ^{13}C (75.4 MHz, CDCl_3): δ 151.3, 149.8, 144.1, 140.8, 133.7, 128.8, 127.4, 126.6, 122.9, 120.1, 118.9, 83.7, 55.1, 40.25, 31.8, 30.0, 29.2, 24.9, 23.7, 22.6, 14.1. MALDI-TOF-MS m/z $[\text{M}+\text{H}]^+$ calcd for $\text{C}_{35}\text{H}_{53}\text{BO}_2$ $[\text{M}+\text{H}]^+$ m/z 516.61; found 516.32.

2-(4-(9,9-Dioctyl-9H-fluoren-2-yl)phenyl)acetonitrile (5): A dry flask (50 mL) was charged with compound 3 (2.94 g, 0.005 mol), 4-bromophenylacetonitrile (1.40 g, 0.006 mol), DME (30 mL) and 2 M sodium carbonate (1.06 g) in inert nitrogen condition. De-gassed the reaction mixture up to 20 min in nitrogen atmosphere followed by addition of $\text{Pd}(\text{PPh}_3)_4$ (10 %) catalyst and reflux the reaction mixture for 12 h at 70 °C. After completion of reaction, the reaction mixture was workup using EtOAc . The combined organic layer was washed with brine and dried over Na_2SO_4 and organic solvents were completely removed by rotary evaporation. The residue was purified by column chromatography using petroleum ether and EtOAc (3:2) as elutes, to afford product-5 yield (1.5 g, 81 %). ^1H NMR (500.1 MHz, CDCl_3): δ 7.75 (d, $J=7.7$ Hz, 1 H), 7.72 (d, $J=6.5$ Hz, 1 H), 7.65 (d, $J=8.2$ Hz, 2 H), 7.54 (d, $J=7.6$ Hz, 1 H), 7.52 (s, 1 H), 7.41 (d, $J=8.3$ Hz, 2 H), 7.35–7.29 (m, 3 H), 3.84 (s, 2 H), 2.07–1.90 (m, 4 H), 1.27–1.12 (m, 6 H), 1.12–0.99 (m, 16 H), 0.80 (t, 6 H). ^{13}C NMR (125.7 MHz, CDCl_3): δ 151.5, 151.0, 141.6, 140.8, 140.6,

138.9, 128.6, 128.3, 127.9, 127.2, 126.8, 125.9, 122.9, 121.4, 120.0, 119.8, 117.9, 55.2, 40.4, 31.8, 30.0, 29.2, 23.8, 23.3, 22.6, 14.1. HRMS (m/z): $[\text{M}+\text{H}]^+$ calcd for $\text{C}_{37}\text{H}_{47}\text{N}$: 505.3704; found 505.3701.

(2E,2'E)-3,3'-(1,4-Phenylene)bis(2-(4-(9,9-dioctyl-9H-fluoren-2-yl)phenyl)acrylonitrile) (7): In a 100 mL of round bottom flask was charged with terephthalaldehyde (100 mg, 0.74 mmol), compound-5 (1.50 g, 0.003 mol) and ethanol (10 mL), after formation of homogeneous solution sodium ethoxide (152 mg, 2.23 mmol) was added. The reaction was stirred at 50 °C for 4 h, after the completion of reaction the crude material was filtered using Buchner funnel and washed with cold ethanol. The crude solid was washed with brine water and dried over Na_2SO_4 . The organic solvent was evaporated using reduced pressure and purified by column chromatography using petroleum ether/DCM (2:3) to afford the product-7 (500 mg, 60 % yield). ^1H NMR (500.1 MHz, CDCl_3): δ 8.05 (s, 2 H), 7.83–7.80 (m, 2 H), 7.80–7.73 (m, 4 H), 7.63–7.59 (m, 3 H), 7.38–7.32 (m, 3 H), 2.04–2.18 (m, 4 H), 1.33–0.99 (m, 24 H), 0.80 (t, 6 H). ^{13}C NMR (125.7 MHz, CDCl_3): δ 151.6, 151.0, 142.9, 141.1, 140.5, 140.0, 138.5, 135.5, 132.8, 129.8, 127.8, 127.2, 126.8, 126.5, 125.9, 122.9, 121.3, 120.1, 119.9, 117.8, 112.6, 55.2, 40.4, 31.8, 30.0, 29.2, 23.8, 22.6, 14.1. HRMS (m/z): $[\text{M}+\text{H}]^+$ calcd for $\text{C}_{82}\text{H}_{96}\text{N}_2$: 1108.7574; found 1108.7571.

9,12-Bis(9,9-dioctyl-9H-fluoren-2-yl)dibenzo[*c,g*]phenanthrene-1,6-dicarbonitrile (9): To a dry toluene solution (100 mL) of compound 7 (100 mg, 0.09 mmol), iodine (92 mg, 0.36 mmol) was added. The solution was irradiated using 400 nm UV-lamp for 48 h. After completion of reaction the crude product was washed with sodium thiosulfate, brine solution and dried over Na_2SO_4 . The organic solution was evaporated under reduced pressure. The residue was purified by column chromatography using petroleum ether/DCM (3:2) to afford the final product-9 as a pale green colour solid (50 mg, 35 % yield). ^1H NMR (500.1 MHz, CDCl_3): δ 8.95 (s, 2 H), 8.60 (d, $J=8.5$ Hz, 2 H), 8.38 (s, 2 H), 8.26 (d, $J=9.5$ Hz, 2 H), 8.0 (s, 2 H), 7.63–7.52 (m, 6 H), 7.24–7.21 (m, 8 H), 1.79–1.66 (m, 8 H), 1.33–1.20 (m, 7 H), 1.11–1.02 (m, 9 H), 0.99–0.78 (m, 32 H), 0.75 (t, 6 H), 0.67 (t, 6 H). ^{13}C NMR (125.7 MHz, CDCl_3): δ 151.8, 150.9, 141.4, 140.1, 139.9, 138.0, 133.6, 132.1, 130.9, 129.2, 129.1, 127.8, 127.7, 127.3, 126.7, 126.4, 126.1, 122.8, 121.4,

120.1, 119.8, 117.3, 110.8, 55.0, 40.1, 40.0, 31.8, 31.6, 30.1, 29.7, 29.3, 29.0, 28.9, 23.9, 23.5, 22.6, 22.5, 14.1, 13.9. HRMS (m/z): $[M+H]^+$ calcd for $C_{82}H_{92}N_2$: 1104.7261; found: 1104.7269.

3-Bromo-9-octyl-9H-carbazole (2): To a dry flask (50 mL) was charged with 3-bromocarbazole (1.0 g, 0.004 mol), K_2CO_3 (2.25 g, 0.016 mol) and DMF (30 mL) under nitrogen gas atmosphere. After stirring for 10 min, 1-bromooctane (2.35 g, 0.012 mol) was slowly added and refluxed at 110 °C for 24 h. After completion of the reaction, the DMF solvent was evaporated by rota evaporator and extracted with EtOAc. The combined organic layer was washed with brine and dried over Na_2SO_4 . The residue was purified by column chromatography using petroleum as eluent, to afford product 2 yield (850 mg, 75 %). 1H NMR (400.1 MHz, $CDCl_3$): δ 8.17 (s, 1 H), 8.01 (d, $J=7.82$ Hz, 1 H), 7.51 (m, 1 H), 7.49 (m, 1 H), 7.43 (m, 1 H), 7.34 (d, $J=8.31$ Hz, 1 H), 7.20 (m, 1 H), 4.19 (t, 2 H), 1.83–1.78 (m, 2 H), 1.35–1.27 (m, 4 H), 1.25–1.15 (m, 6 H), 0.85 (t, 3 H). ^{13}C (75.4 MHz, $CDCl_3$): δ 140.7, 139.0, 128.2, 126.3, 124.5, 123.0, 121.8, 120.5, 119.2, 111.5, 110.0, 108.9, 43.4, 31.8, 29.4, 29.2, 28.9, 27.322.6, 14.1. MALDI-TOF-MS m/z $[M+H]^+$ calcd for $C_{20}H_{24}BrN$ $[M+H]^+$ m/z 358.11; found 358.83.

9-Octyl-3-(4,4,5,5-tetramethyl-1,3,2-dioxaborolan-2-yl)-9H-carbazole (4): A dry flask (50 mL) was charged with compound 2 (950 mg, 2.65 mmol), Bis(pinacolato)diboron (876 mg, 3.44 mmol) and KOAc (1.60 g, 0.015 mol) in dry 1,4-dioxane (40 mL), after de-gassed for 20 min $Nd(dppf)Cl_2$ (10 %) was added. The reaction mixture was stirred under nitrogen atmosphere at 100 °C for 24 h. After cooling to room temperature, the solvent was removed under reduced pressure. The residue was purified by column chromatography on silica gel with petroleum ether/ethyl acetate (2:3) to afford the product 4 as colour less liquid yield (780 mg, 69 %). 1H NMR (500.1 MHz, $CDCl_3$): δ 8.60 (s, 1 H), 8.13 (d, $J=7.7$ Hz, 1 H), 7.92 (d, $J=9.4$ Hz, 1 H), 7.50–7.43 (m, 1 H), 7.40 (d, $J=8.9$ Hz, 2 H), 7.20–7.22 (m, 1 H), 4.29 (m, 2 H), 1.89–1.82 (m, 2 H), 1.40 (s, 12 H), 1.35–1.27 (m, 4 H), 1.25–1.16 (m, 6 H), 0.85 (t, 3 H). ^{13}C (75.4 MHz, $CDCl_3$): δ 142.6, 139.7, 132.2, 127.7, 125.6, 123.1, 122.6, 120.6, 119.2, 108.7, 108.1, 83.6, 43.1, 31.8, 29.4, 29.1, 28.9, 27.3, 24.9, 22.6, 14.1. MALDI-TOF-MS m/z $[M+H]^+$ calcd for $C_{26}H_{36}BNO_2$ $[M+H]^+$ m/z 405.38; found 405.10.

2-(4-(9-Octyl-9H-carbazol-3-yl) phenyl)acetonitrile (6): To a dry flask (50 mL) compound 4 (780 mg, 1.92 mmol), 4-bromophenylacetonitrile (453 mg, 2.30 mmol), DME (30 mL) and 2 M sodium carbonate (1.06 g) was added under inert nitrogen condition. De-gassed the reaction mixture for 20 min in nitrogen atmosphere then added $Pd(PPh_3)_4$ (10 %) catalyst and refluxed 12 h at 70 °C. After completion of the reaction, the reaction mixture was workup by using EtOAc. The combined organic layer was washed with brine and dried over Na_2SO_4 . The residue was purified by column chromatography using petroleum and EtOAc (3:2) to afford product-6 yield (1.17 g 81 %). 1H NMR (500.1 MHz, $CDCl_3$): δ 8.28 (s, 1 H), 8.13 (d, $J=7.7$ Hz, 1 H), 7.70 (d, $J=8.2$ Hz, 2 H), 7.66 (d, $J=7.4$ Hz, 1 H), 7.47 (t, $J=5.7$ Hz, 1 H), 7.44 (s, 1 H), 7.41 (d, $J=7.0$ Hz, 1 H), 7.37 (d, $J=4.8$ Hz, 2 H), 7.24 (d, $J=8.3$ Hz, 1 H), 4.28 (t, 2 H), 3.76 (s, 2 H), 1.89–1.83 (m, 2 H), 1.40–1.31 (m, 4 H), 1.25–1.23 (m, 6 H), 0.86 (t, 3 H). ^{13}C (75.4 MHz, $CDCl_3$): δ 142.0, 140.9, 140.1, 132.3, 131.1, 129.6, 128.4, 127.9, 125.9, 125.0, 123.4, 122.9, 120.4, 119.0, 118.8, 118.0, 109.0, 108.9, 43.2, 31.8, 29.4, 29.2, 29.0, 27.3, 23.3, 22.6, 14.1. HRMS (m/z): $[M+H]^+$ calcd for $C_{28}H_{30}N_2$: 394.240; found 394.241.

(2E,2'E)-3,3'-(1,4-Phenylene)bis(2-(4-(9-octyl-9H-carbazol-3-yl) phenyl)acrylonitrile) (8): To a 50 mL of dry round bottom flask charged with terephthalaldehyde (100 mg, 0.74 mmol), compound-6 (1.17 g, 0.002 mol) and ethanol (10 mL), after formation of homogeneous solution sodium ethoxide (152 mg, 2.23 mmol) was added. The reaction contents were stirred under inert atmosphere at 50 °C for 4 h, after the completion of reaction the crude material was filtered by Buchner funnel and washed with cold ethanol. The crude solid was washed with brine solution and dried over sodium sulphate. The organic solvent was evaporated under reduced pressure and purified by column chromatography using petroleum ether/DCM (2:3) to afforded the product-8

yield (100 mg, 60 % yield). 1H NMR (500.1 MHz, $CDCl_3$): δ 8.36 (s, 2 H), 8.17 (d, $J=7.5$ Hz, 2 H), 8.04 (s, 3 H), 8.01–7.99 (m, 1 H), 7.82 (s, 6 H), 7.77–7.74 (m, 3 H), 7.62–7.58 (m, 3 H), 7.53–7.48 (m, 5 H), 7.45–7.42 (m, 2 H), 7.26 (m, 1 H), 4.34 (t, 4 H), 1.93–1.88 (m, 4 H), 1.43–1.31 (m, 8 H), 1.25–1.23 (m, 12 H), 0.87 (t, 6 H). ^{13}C (75.4 MHz, $CDCl_3$): δ 143.5, 141.0, 140.9, 140.8, 140.3, 139.5, 135.4, 134.9, 132.8, 129.8, 129.8, 127.7, 127.5, 126.5, 126.0, 124.9, 123.4, 122.8, 120.4, 119.1, 118.8, 109.1, 108.9, 43.3, 31.8, 29.7, 29.4, 29.2, 27.3, 22.6, 14.0. HRMS (m/z): $[M+H]^+$ calcd for $C_{64}H_{62}N_4$: 886.4974; found 886.4971.

9,12-Bis(9-octyl-9H-carbazol-3-yl)dibenzo[*c,g*]phenanthrene-1,6-dicarbonitrile (10): To a toluene solution (120 mL) of compound 8 (100 mg, 0.10 mmol), iodine (115 mg, 0.40 mmol) was added. The solution was irradiated by 400 nm UV-lamps for 64 h, after completion of reaction mixture. The crude material was washed with sodium thiosulfate and brine solution dried over Na_2SO_4 . The organic solvent was evaporated under reduced pressure. The residue was purified by column chromatography using petroleum/DCM (3:2) to afford the final product-10 as an orange colour solid yield (50 mg, 35 %). 1H NMR (500.1 MHz, $CDCl_3$): δ 8.37 (s, 2 H), 8.18 (d, $J=7.5$ Hz, 2 H), 8.05 (s, 4 H), 7.83 (m, 6 H), 7.76 (d, $J=8.4$ Hz, 2 H), 7.63 (s, 2 H), 7.50 (d, $J=8.3$ Hz, 2 H), 7.44 (d, $J=8.1$ Hz, 2 H), 4.34 (t, 4 H), 1.94–1.87 (m, 4 H), 1.48–1.34 (m, 8 H), 1.28–1.23 (m, 12 H), 0.86 (t, 6 H). ^{13}C (75.4 MHz, $CDCl_3$): δ 143.4, 140.9, 140.2, 139.7, 139.3, 135.5, 132.3, 132.1, 130.7, 129.7, 127.7, 126.5, 126.0, 124.9, 123.4, 122.9, 120.5, 119.1, 118.8, 117.9, 114.1, 112.6, 109.1, 108.9, 43.2, 31.9, 31.8, 29.4, 29.0, 27.3, 22.6, 14.1. HRMS (m/z): $[M+H]^+$ calcd for $C_{64}H_{58}N_4$: 883.4692; found 883.4690.

Absorption spectra of FLU-HEL and CBZ-HEL (Fig. 2a) [5]helicene dyes were studied in dichloromethane solution with concentration of 0.02 mol/L, both dyes displayed two peaks in higher energy region (287, 319 nm and 288, 356 nm respectively) and one peak in the lower energy region (431 and 415 nm respectively). The broad absorption at the lower energy is associated with the intramolecular charge transitions between the strong electron acceptor cyano (-CN) groups and strong electron donor fluorene and carbazole moiety. The parent compounds FLU-TPD and CBZ-TPD show similar absorption pattern as the final dyes (see Scheme 1, Fig. S1a in the Supporting Information (SI)). FLU-HEL and CBZ-HEL dyes shows 20 nm red shift from their precursor FLU-TPD and CBZ-TPD compounds due to increase in the electronic conjugation within the molecule. Further we have extended our study to thin film. Both the [5]helicene dyes show ~5–20 nm red shift compared to the absorption in solution (Fig. S1b), which might be attributed to strong intermolecular π - π stacking interaction, exists between the molecular backbones in the solid film. The optical band gaps of films were estimated from the onset of absorption to be ~2.0–2.5 eV (Table S1 in SI).

To better understand the excitation and intramolecular charge transfer for the synthetic [5]helicene dyes, we have performed the fluorescence emission spectra for both FLU-HEL and CBZ-HEL dyes in dry dichloromethane at room temperature with concentration of 0.02 mg mL⁻¹ (Fig. 2b). We have observed the broad emission in the region ~ 400–750 nm with a single emission maximum at 475 and 581 nm for FLU-HEL and CBZ-HEL respectively. Literature review suggests that the substitution on the most stable [5]helicene aromatic moiety influences the fluorescence emission of dyes. Here, in the case of CBZ-HEL we observed more than 100 nm red shift in fluorescence emission compared to FLU-HEL due to the presence of carbazole moiety, a strong electron donor. A subtle effect on the molecular absorption spectra and also a noticeable change on the fluorescence emission spectra might be occurring due to change of structures in the ground state and excited state [14,16–17].

We have calculated the photoluminescence quantum yield (QY) by using standard anthracene dye as a reference having QY of 27 % in EtOH. The QY of FLU-HEL and CBZ-HEL was found to be 27 % and 30 % respectively and the relevant data is summarized in Table S1. The high QY in CBZ-HEL arises probably due to strong electron donating character of carbazole unit. The average life-time decay for FLU-HEL and CBZ-HEL dyes was found to be in order of 9.72 and 4.28 ns respectively.

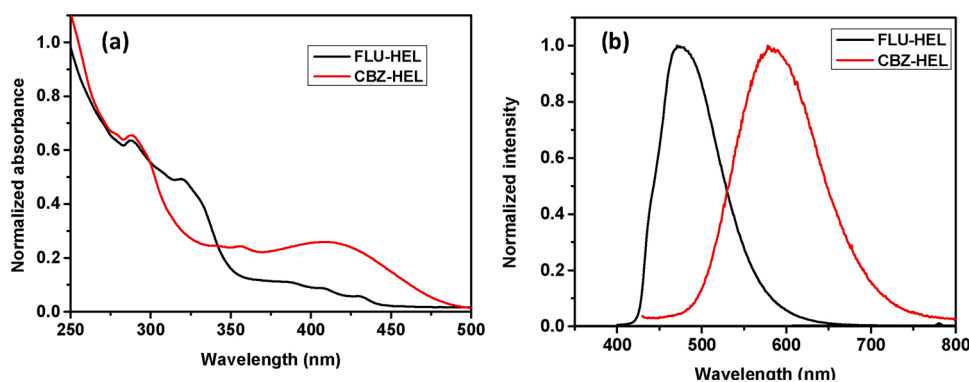


Fig. 2. Normalized UV-vis absorption (a) and fluorescence (b) spectra of FLU-HEL and CBZ-HEL in dichloromethane with concentration of 0.02 mol/L.

The radiative and non-radiative decay constant for both the dyes were calculated (Table S2 in SI). These findings demonstrate that the 2,12-disubstituted [5]helicene dyes such as FLU-HEL and CBZ-HEL display large Stokes shifts and high quantum yields. Both dyes showed a significant variation in its photophysical properties just by the changing substituent on stable [5]helicene core. We have also investigated the variation of the fluorescence properties in dichloromethane under different wavelength of exciting light (Fig. S2 in SI), which

unambiguously demonstrated their fluorescence variation.

Fig. 3a and b display the absorption and emission spectra of both the dyes in various solvents. The absorption spectra are insensitive towards the solvatochromic effect which implies that the ground state is less polar (see Table S3 and S4 in the Supporting Information). However, the emission spectra of both dyes were sensitive to the solvent polarity indicating a moderate positive solvatochromic shift upon increasing the solvent polarity. The results suggest that the excited states of both

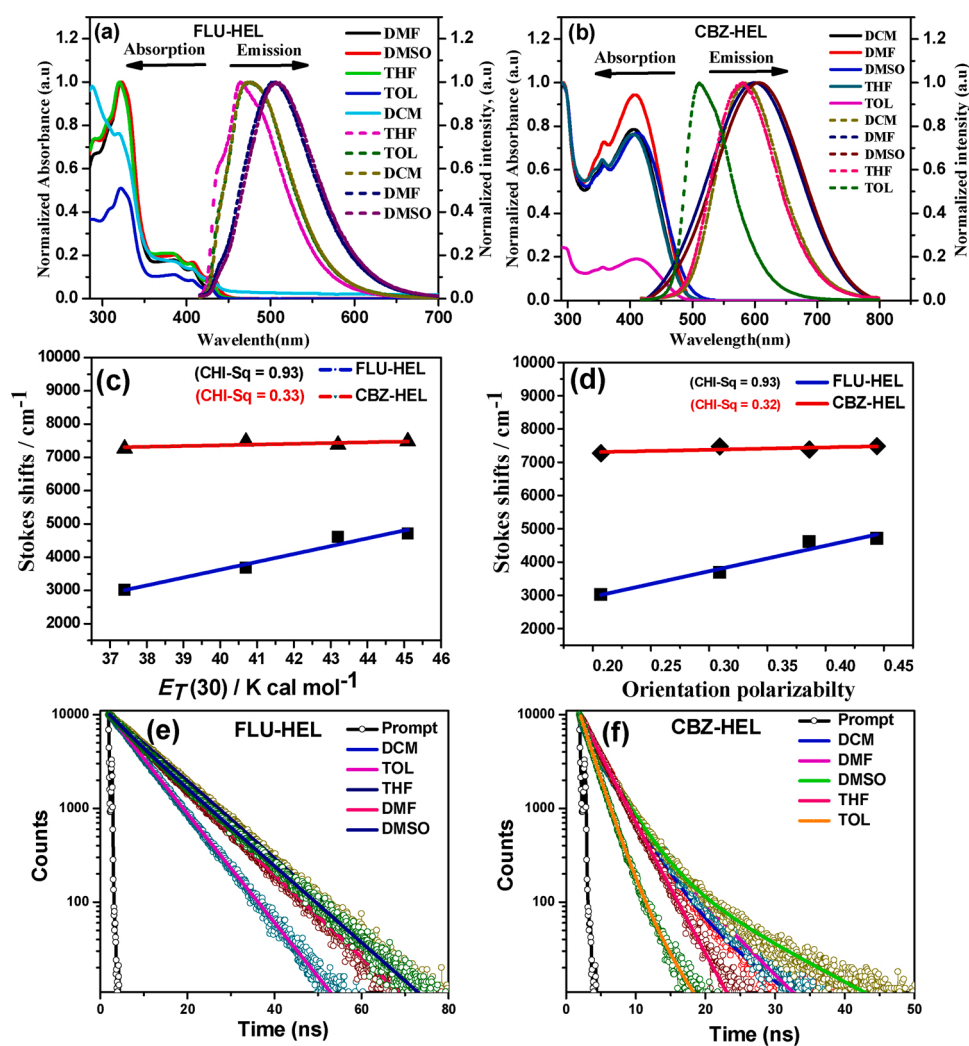


Fig. 3. a) and b) Normalized UV-vis absorption and emission spectra of FLU-HEL and CBZ-HEL in different solvents with concentration of 0.02 mg mL⁻¹, (c) Stokes shift versus $E_T(30)$ and (d) Lippert – Mataga plots for the dyes and (e) time-correlated single photon counting (TCSPC) analysis for FLU-HEL and (f) for CBZ-HEL in different solvents.

molecules are more polar than their ground states [10].

Interestingly, FLU-HEL exhibited poor sensitivity towards solvatochromic shift and indicates a poor polar $\pi\text{-}\pi^*$ excited states. Whereas, CBZ-HEL contains carbazole chromophore, a strong electron donor, thus exhibiting positive solvent induced emission shift, which reflects the stabilization of the excited states in polar solvents. However, both molecules showed a significant dipolar character in the excited states but not in the ground state [18]. The positive solvatochromic shift for both dyes might be due to intramolecular charge transfer between the excited states from donor molecules (fluorene, carbazole) to acceptor cyano group.

Though, the extent charge transmission is restricted in FLU-HEL as it is evident from the smaller value of bathochromic shift with increasing solvent polarity from TOL to DMSO ($\Delta\lambda_{\text{em}} = \sim 30$ nm) [18]. Generally, the charge transfer in bipolar compounds is associated with large Stokes shifts difference between non-polar (TOL) and the polar solvent (DMSO) [19], as is the case with CBZ-HEL ($\lambda_{\text{em}} = \sim 100$ nm) red shifted from TOL to DMSO. Unexpectedly the dyes showed a strong red shift in high polar DMSO solution. Mostly, this kind of behaviour has been observed in organic fluorophores and can be attributed to the instant stabilization of polarizable electrons during electronic excitation [20]. The fluorescence alterations of both dyes in five different solvents were showed in presence of different wavelength of light (UV-light and fluorescence light) (see Fig. S3 in the SI).

FLU-HEL and CBZ-HEL [5]helicene dyes showed solvent dependent excited state properties which is further supported by Lippert-Mataga and Stokes shift *versus* $E_{\text{T}}(30)$ correlations. We have observed nearly linear movements in Fig. 3c & d with sharper slopes for both dyes, which explain a general solvent effect for the dyes in the excited state. The dye CBZ-HEL displays a large change in Stokes shift ($\lambda_{\text{em}} - \lambda_{\text{ab}}$) confirming most prominent intramolecular charge transfer in the excited state. The lifetime study for the [5]helicene dyes in different solvent is shown in Fig. 3e and f and the supporting data is given in Table S5. As the polarity of the solvent is increasing the average life time of both the dyes is increasing due to high solubility and stable excited state.

The HOMO energy levels were calculated to be -5.60 eV and -5.17 eV for FLU-HEL and CBZ-HEL respectively (briefly discussed in the SI; see Fig. S4, Table S6). We have observed the fluorescence behaviour using different metal salts for sensing the metals (see Fig. S6 in the SI). The UV-vis absorption spectra (see Fig. S5 in the SI) and fluorescence emission spectra of FLU-HEL and CBZ-HEL with different metal salts (see Fig. S7a and S7e in the SI) showed drastic change in absorbance as well as fluorescence. Particularly in the case of Fe^{3+} metal salt both absorbance and emission were quenched. The interaction of Fe^{3+} ion with FLU-HEL and CBZ-HEL dyes results in increase in absorption and quenching of fluorescence. The quenching in fluorescence is related to non-radiative electron transfer, which involves the partial transfer of an electron from the excited state of FLU-HEL and CBZ-HEL [5]helicene dyes to the d orbital of Fe^{3+} transition metal ion.

The fluorescence intensity of both FLU-HEL and CBZ-HEL [5]helicene dyes decreases gradually on successive addition of Fe^{3+} ion with concentration in the range of 0–426 micromolar (μM) (see Fig. S7b and S7f in the SI), which reveals that Fe^{3+} metal ion is coordinating with both dyes and reduce the fluorescence so it can be used as a fluorescent probe for Fe^{3+} metal ion detection [12]. Difference in fluorescence intensity of [5]helicene dye is proportional to Fe^{3+} ion concentration so it was well explained by the Stern–Volmer relationship (see Fig. S7c and S7g in the SI). This gives a linear regression equation with K_{SV} equal to $6.6 \times 10^3 \text{ L mol}^{-1}$ and $5.3 \times 10^3 \text{ L mol}^{-1}$ and the correlation coefficients of 0.98 and 0.99 for FLU-HEL and CBZ-HEL respectively. We have observed the linearity till the 426 μM concentration for CBZ-HEL.

We have briefly discussed the quenching phenomenon of both dyes using K_{SV} values, Stern-Volmer plots and TCSPC etc. are discussed in the Supporting Information (see Fig. S5 and S7, Table S7 in the SI). Furthermore, we have extended our study to security purpose. Both FLU-

HEL and CBZ-HEL can be used as a fluorescent ink under excitation at 365 nm, and can also replace traditional inks for security purposes. We have chosen the commercially available paper because it is non-fluorescent under 365 nm excitation. Initially, we have refilled the pen refill with the FLU-HEL and CBZ-HEL fluorescent dyes shown in Fig. 4d and used for hand writing purpose on paper. We observed that hand-written paper under excitation at 365 nm show the written text and in day light condition it looks like blank paper (Fig. 4c and e). Further, silica gel mesh used for TLC purpose does not show any fluorescence under excitation at 365 nm. When the FLU-HEL and CBZ-HEL dyes were adsorbed on it starts to show the fluorescent (Fig. 4a and b). These are few basic experiments which can be used for the forensic and security purpose.

The circular dichroism (CD) spectrum was obtained in a chloroform solution (1×10^{-5} M) for the both FLU-HEL and CBZ-HEL [5]helicene molecules (Fig. 5). CBZ-HEL displayed a maximum at 303 nm ($\Delta\epsilon = 77 \text{ M}^{-1} \text{ cm}^{-1}$) attributable to the central helicene moiety and a minimum at 473 nm ($\Delta\epsilon = 111 \text{ M}^{-1} \text{ cm}^{-1}$) most likely due to the synergistic combination of the inherent chirality of [5]helicene with the strong absorptivity of the carbazole chromophores [20]. The corresponding peaks in FLU-HEL were at 318 nm ($\Delta\epsilon = 80 \text{ M}^{-1} \text{ cm}^{-1}$) and 488 nm ($\Delta\epsilon = 76 \text{ M}^{-1} \text{ cm}^{-1}$) respectively. These observations confirm the inherently chirality and efficient transference of chirality throughout the molecules. The theoretical geometry study of both FLU-HEL and CBZ-HEL dyes were briefly studied by using B3LYP exchange correlations functional with 6–311 g (d, p) as a basis set and the optimized structures were showed in supporting information (Fig. S8). To present some insight into experimentally observed photophysical properties of FLU-HEL and CBZ-HEL [5]helicene dyes, TDDFT calculations were performed under the same basis set and briefly discussed in supporting information (Fig. S9–S11), the corresponding data were tabulated in table S8.

3. Conclusions

In summary, we have designed and synthesized two new fluorene (FLU-HEL) and carbazole (CBZ-HEL)-based 2,12-disubstituted [5]helicene *via* photochemical reaction. Both the [5]helicene dyes exhibited very intense fluorescence property and fluorescence quantum yield $\Phi_{\text{f}} = 27\%$ and 30% and life time ($\langle\tau_{\text{f}}\rangle = 9.7$ ns and 4.2 ns) was observed. Both [5]helicenes are highly sensitive towards Fe^{3+} transition metal ion, than other transition metal ions. Therefore; these organic dyes can be utilized as Fe^{3+} ion sensors. Furthermore, another interesting features of these [5]helicene for security application was explored. A successful

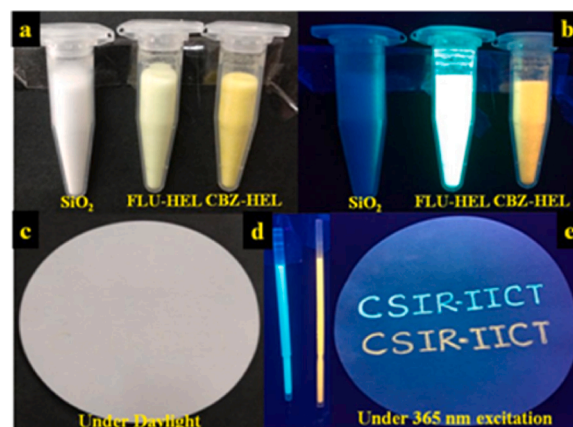


Fig. 4. a) SiO_2 , $\text{SiO}_2 + \text{FLU-HEL}$, $\text{SiO}_2 + \text{CBZ-HEL}$ under daylight. b) SiO_2 , $\text{SiO}_2 + \text{FLU-HEL}$, $\text{SiO}_2 + \text{CBZ-HEL}$ under 365 nm excitation c) Handwritten paper with FLU-HEL and CBZ-HEL dyes under daylight d) Pen refill filled with FLU-HEL and CBZ-HEL dyes solution e) Handwritten paper with FLU-HEL and CBZ-HEL dyes under 365 nm excitation.

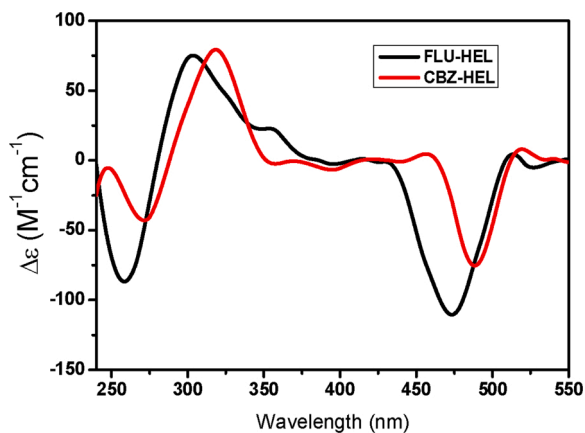


Fig. 5. Circular dichroism (CD) spectrum of FLU-HEL and CBZ-HEL molecules in a chloroform solution with 1×10^{-5} M concentration.

demonstration was displayed to formulate fluorescent ink and its refilling. This study allows developing a variety of materials for sensing, and security applications.

Author statement

All the authors are aware and agreed about this publication. All the information provided in this article is correct.

Notes

The authors declare no competing financial interest.

Declaration of Competing Interest

The authors declare no conflict of interest.

Acknowledgements

BYG thanks UGC for providing senior research fellowship. SPS acknowledges financial support from DST-SERB (EMR/2017/001506). We also thank CSIR for the FBR project (Ref. No. 34/1/TD-CLP/NCP-FBR 2020-RPPBDD-TMD-Se-MI). IICT Communication No.: IICT/Pubs./2018/167.

Appendix A. Supplementary data

Supplementary material related to this article can be found, in the online version, at doi:<https://doi.org/10.1016/j.jphotochem.2021.113203>.

References

- [1] M. Gingras, G. Félix, R. Peresutti, One hundred years of helicene chemistry. Part 2: stereoselective synthesis and chiral separations of carbohelicenes, *Chem. Soc. Rev.* 42 (2013) 1007–1050.
- [2] A. Urbano, Recent developments in the synthesis of helicene-like molecules, *Angew. Chem. Int. Ed.* 42 (2003) 3986–3989.
- [3] Y. Shen, C.-F. Chen, Helicenes: synthesis and applications, *Chem. Rev.* 112 (2012) 1463–1535.
- [4] T.E. Kaiser, H. Wang, V. Stepanenko, F.W. Wurthner, Supramolecular construction of fluorescent j-aggregates based on hydrogen-bonded perylene dyes, *Angew. Chem., Int. Ed.* 46 (2007) 5541–5544.
- [5] N. Hoffmann, Photochemical reactions applied to the synthesis of helicenes and helicene-like compounds, *J. Photochem. and Photobiol. C-Photochem. Rev.* 19 (2014) 1–19.
- [6] W.-L. Zhao, M. Li, H.-Y. Lu, C.-F. Chen, Advances in helicene derivatives with circularly polarized luminescence, *Chem. Commun.* 55 (2019) 13793–13803.
- [7] (a) S. Yang, J. You, J. Lan, Facile access to extremely efficient energy-transfer pairs via an unexpected reaction of squaraines with ketones, *J. Am. Chem. Soc.* 134 (2012) 11868–11871; (b) C. Vijayakumar, K. Sugiyasu, M. Takeuchi, Oligofluorene-based electrophoretic nanoparticles in aqueous medium as a donor scaffold for fluorescence resonance energy transfer and white-light emission, *Chem. Sci.* 2 (2011) 291–294.
- [8] (a) M. Rickhaus, M. Mayor, M. Juriček, Strain-induced helical chirality in polyaromatic systems, *Chem. Soc. Rev.* 45 (2016) 1542–1556; (b) M. Gingras, One hundred years of helicene chemistry. Part 1: non-stereoselective syntheses of carbohelicenes, *Chem. Soc. Rev.* 42 (2013) 968–1006.
- [9] M. Li, W. Yao, J.D. Chen, H.Y. Lu, Y.S. Zhao, C.F. Chen, Tetrahydro[5]helicene-based full-color emission dyes in both solution and solid states: synthesis, structures, photophysical properties and optical waveguide applications, *J. Mater. Chem. C Mater. Opt. Electron. Devices* 2 (2014) 8373–8380.
- [10] Y. Sawada, S. Furumi, A. Takai, M. Takeuchi, K. Noguchi, K. Tanaka, Rhodium-catalyzed enantioselective synthesis, crystal structures, and photophysical properties of helically chiral 1,1'-bitriphenylenes, *J. Am. Chem. Soc.* 134 (2012) 4080.
- [11] L. Cai, X. Sun, W. He, R. Hu, B. Liu, J. Shen, A solvatochromic AIE tetrahydro[5]helicene derivative as fluorescent probes for water in organic solvents and highly sensitive sensors for glycerylmonostearate, *Talanta* 206 (2020), 120214.
- [12] X.-H. Gu, Y. Lei, S. Wang, F. Cao, Q. Zhang, S. Chen, K.-P. Wang, Z.-Q. Hu, Tetrahydro[5]helicene fused nitrobenzoxadiazole as a fluorescence probe for hydrogen sulfide, cysteine/homocysteine and glutathione, *Spectrosc. Acta Part A-Mol. Biomol. Spectrosc.* 229 (2020), 118003.
- [13] A. Petduma, N. Waraeksiria, O. Hanmenga, S. Jarutikorna, S. Chaneama, J. Siriraka, A. Charoenpanich, W. Panchan, T. Sooksimuang, N. Wanichachev, A new water-soluble Fe³⁺ fluorescence sensor with a large Stokes shift based on [5]helicene derivative: its application in flow injection analysis and biological systems, *J. Photochem. Photobiol. A-Chem.* 401 (2020) 112769.
- [14] H. Takashi, I. Natsuki, K. Hiromu, S. Tohru, K. Matsuda, Fluorescence behaviour of 5,10-disubstituted [5]helicene derivatives in solution and the effect of self-assembly on their radiative and non-radiative rate constants, *J. Mater. Chem. C* 4 (2016) 2811–2819.
- [15] W. Hua, Z. Liu, L. Duan, G. Dong, Y. Qiu, B. Zhang, D. Cui, X. Tao, N. Cheng, Y. Liu, Deep-blue electroluminescence from non-doped and doped organic light-emitting diodes (OLEDs) based on a new monoaza[6]helicene, *RSC Adv.* 5 (2015) 75–84.
- [16] Y. Hu, B. Wex, M.W. Perkovic, D.C. Neckers, Tunable blue-emitting fluorophores-benzo[1,2-*b*:4,3-*b'*]dithiophene and trithia[5]helicene end-capped with electron-rich or electron-deficient aryl substituents, *Tetrahedron* 64 (2008) 2251–2258.
- [17] M. Li, Y. Niu, X. Zhu, Q. Peng, H.Y. Lu, A. Xia, C.F. Chen, Tetrahydro[5]helicene-based imide dyes with intense fluorescence in both solution and solid state, *Chem. Commun.* 50 (2014) 2993–2995.
- [18] K. Rajendra Kumar, K.R. Justin Thomas, S. Sahoo, D. Deepak Kumar, J.H. Joub, Multi-substituted deep-blue emitting carbazoles: a comparative study on photophysical and electroluminescence characteristics, *J. Mater. Chem. C* 5 (2017) 709–726.
- [19] R.K. Konidena, K.R. Thomas, S. Kumar, Y.C. Wang, C.J. Li, J.H. Jou, Phenothiazine decorated carbazoles: effect of substitution pattern on the optical and electroluminescent characteristics, *J. Org. Chem.* 80 (2015) 5812–5823.
- [20] N.J. Schuster, D.W. Paley, S. Jockusch, F. Nag, M.L. Steigerwald, C. Nuckolls, Electron delocalization in perylene diimide helicenes, *Angew. Chem. Int. Ed.* 55 (2016) 13519–13523.
- [21] Y. Wen, F. Huo, C. Yin, Organelle targetable fluorescent probes for hydrogen peroxide, *Chin. Chem. Lett.* 30 (2019) 1834–1842.
- [22] W. Zhang, F. Huo, C. Yin, Photocontrolled single-/dual-site alternative fluorescence probes distinguishing detection of H₂S/SO₂ in Vivo, *Org. Lett.* 21 (2019) 5277–5280.
- [23] J. Cui, Y. Yao, C. Chen, R. Huang, W. Zhang, J. Qian, Mitochondria-targeted ratiometric fluorescent probes for micropolarity and microviscosity and their applications, *Chin. Chem. Lett.* 30 (2019) 1071–1074.